Polymer 50 (2009) 1602–1608

Contents lists available at ScienceDirect

Polymer

journal homepage: www.elsevier.com/locate/polymer

Affinity adsorption mechanism studies of adsorbents for oligopeptides using model polymer

Jihong Li, Jing Feng, Qinqin Dang, Yitao Qiao, Jianxin Zhao, Saihui Zhang, Hongwei Sun, Xin Wen, Zhi Yuan*

College of Chemistry, Key Laboratory of Functional Polymer Materials, Ministry of Education, Nankai University, Tianjin 300071, China

ARTICLE INFO

Article history:
Received 8 September 2008
Received in revised form
17 November 2008
Accepted 9 January 2009
Available online 20 January 2009

Keywords:
Oligopeptide
Affinity adsorption mechanism
Adsorbent

ABSTRACT

To understand the principle of designing efficient adsorbents toward specific peptides, adsorption mechanism between oligopeptide VVRGCTWW (VW-8) and alkylamine modified polyacrylamide adsorbents was studied in this article. Linear models of the adsorbents were used to facilitate various measurements except for adsorption experiment. 2D ^{1}H NMR experiments reveal the main binding site of VW-8 to the adsorbents is C-terminal Trp. When peptide CTWW (CW-4) was introduced as the reference, the same binding site was found. However, in adsorption experiments, a remarkable difference was observed with the adsorption capacity of the two peptides. According to isothermal titration calorimetry (ITC) and surface plasmon resonance (SPR) experiments, which are in good agreement with the adsorption results, VW-8 has much higher affinity to the adsorbents than CW-4 and the main driving force in adsorption process is considered to be electrostatic force. However, the unusual affinity adsorption of two oligopeptides on the adsorbents contrasted to the traditional view of electrostatic interaction. With a comprehensive understanding of above experimental results along with computer-aided analysis, we conclude that the difference in conformation of the two peptides has a great impact on the interaction mode and further affects the affinity between the peptides and the adsorbents. This provides valuable information for the further design of synthetic affinity ligand for VW-8.

1. Introduction

Since the affinity adsorbents used for purification of staphylococcal nuclease was first reported in 1968 [1], affinity adsorbents have been one of the most effective and powerful materials for purification of proteins and peptides [2,3]. In addition, affinity adsorbents are used in blood purification for selective elimination of toxins in patients, for example, removing low-density lipoprotein by adsorbents with sulfonic and cholesterol groups [4]. In recent years the design of affinity materials has been focused on higher affinity and lower cost [5,6]. To date, obtaining high specific adsorbents is mainly achieved via two methods. One is introducing affinity ligands on matrix for recognizing the targets; the other is called molecular imprinted technology, which is synthesizing cross-linking polymers as artificial receptors for the targets. Whatever either of methods is chosen, the ideal affinity adsorbents should have the following features; inexpensive, scaleable, durable, highly specific and reusable over multiple cycles [2]. Obviously, the efficient bioaffinity adsorbents, which attain molecular recognition properties with immobilizing the bioactive substance on it, could not meet the above criteria due to its low structural stability and high cost [7]. In contrast, synthetic ligand and molecular imprinted polymer can overcome the drawback of bioaffinity adsorbents. However, despite some molecular imprinted polymers have been applied to recognize proteins or peptides successfully, the obstacle of preparation of these materials for proteins and peptides is remarkable [8]. Using small synthetic ligands is another method for obtaining affinity adsorbents. This type of ligands mainly includes short peptides [9–13], dyes [14–17] and immobilized metals [18,19].

According to the principle of "lock–key", selectivity and specificity of the adsorbents depend on the functional groups on the adsorbents that match the appropriate geometric organization of reciprocal functionality on the target molecule. The evaluation of the selectivity of adsorbents is usually based on the distinct adsorption capacity or retention time on the chromatography of target peptides and reference peptides. To our knowledge, the detailed adsorption mechanism for selectivity between the target and the reference is to some extent neglected. This phenomenon

* Corresponding author. Tel.: +86 22 23501164; fax: +86 22 23503510.
E-mail address: zhiy@nankai.edu.cn (Z. Yuan).

0032-3861/$ – see front matter © 2009 Elsevier Ltd. All rights reserved.
doi:10.1016/j.polymer.2009.01.030

results from two reasons. One is that the mechanism is so clear that it need not to confirm, for example peptide–metal interaction. The other is limited by the complex structure of cross-linking adsorbents, because it is difficult to investigate mechanism on a molecular level due to its insolubility. Moreover, the essential adsorption mechanism has been considered when adsorbents are designed, so the aim of the research usually focuses on obtaining a corresponding adsorbent. In fact, the reference peptides with similar molecular weight, or p*I*, or shape, or similar molecular structure are often chosen [20,21]. That means the difference between target and reference has been projected previously. However, due to numerous unknown factors, the initial design of adsorbents maybe exist the limitation. So choosing some reference peptides to investigate the adsorption mechanism in detail is necessary. It could provide some valuable information to design high affinity adsorbent, especially when few well-known molecular recognition information of target could be consulted.

Peptide VW-8 (NH_2–VVRGCTWW–COOH) accumulated in uremic sera is one of the middle-molecular peptides expected to be removed by affinity adsorbent in hemoperfusion [22]. In our previous work, dimethylamine modified cross-linked polyacrylamide adsorbents DMAPAM (Fig. 1) exhibited certain affinity to VW-8, and the main binding site was found to be tryptophan on the C-terminus by NMR [23]. In the present study, the detailed adsorption mechanism between VW-8 and DMAPAM was investigated by ITC, SPR and computer simulation, and the peptide CW-4 (NH_2–CTWW–COOH), a fragment of VW-8 also possessing tryptophan on the C-terminus, was selected as a reference.

As mentioned above, although surface plasmon resonance (SPR), isothermal titration calorimeter (ITC) and high-resolution NMR spectroscopy have been proved to be powerful methods for studying molecular interactions, these tools do not readily cope with the high rigid cross-linked structures of adsorbents. For this reason, detailed studies of interactions between adsorbents and peptides at a molecular level are necessary to pursue with model systems. So in this paper dimethylamine modified linear polyacrylamide (*l*-DMAPAM) was prepared. The linear polymer *l*-DMAPAM is soluble in H_2O and can serve as an efficient model for the cross-linked adsorbent DMAPAM. The interaction mechanism studied in detail could provide useful information to design more effective adsorbents to remove middle-molecular peptides.

2. Materials and methods

All reagents and chemicals were obtained from common commercial sources and used without further purification unless otherwise noted. Acrylamide was recrystallized from acetone. Peptides VW-8 and CW-4 were purchased from GL Biochem (Shanghai) Ltd.

2.1. Preparation of linear polydimethylamide by precipitation polymerization

To a solution of acrylamide (10 g) in anhydrous ethanol (200 mL) at 60 °C under N_2 was added AIBN (0.2 g) and the solution was maintained at 60 °C for 4 h before filtration. The linear PAM was washed thoroughly with anhydrous ethanol and dried under vacuum at room temperature. The number-average molecular weight was determined to be 2.5×10^4 by gel permeation chromatography.

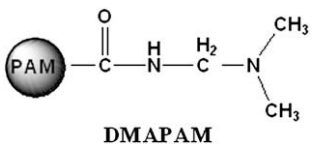

Fig. 1. Structure of DMAPAM.

2.2. Dimethylamine modification of linear PAM

l-DMAPAM was prepared from linear polyacrylamide. Linear PAM (3 g) was dissolved in distilled water (100 mL) at 50 °C before the addition of formaldehyde (36% aqueous solution, 3 mL, 42.5 mmol) and dimethylamine (42.5 mmol). The mixture was kept at 50 °C for 8 h, concentrated under vacuum and acetone was added. The modified linear PAM was filtered, washed with acetone and finally dried under vacuum at 30 °C for 48 h. *l*-DMAPAM: ^{1}H NMR (400 MHz, D_2O) δ 3.8 (br, N–CH_2–N), 2.1 (s, CH_3), 2.0 (br, CH), 1.4 (br, CH_2); average dimethylamine loading, 26%.

2.3. Adsorption experiment of peptides

The static adsorption experiment was carried out according to the method in Ref. [23]. The initial concentrations of both peptides are 100 mM.

2.4. Measurement of isoelectric point

Zeta potentials were measured on a ZetaPlus (Brookhaven Instruments Company) apparatus at 20 °C. The pH values were adjusted with KOH or HCl by autotitration. Water was purified by a MilliQ Plus 185 system. For *l*-DMAPAM, a stock aqueous solution (1.0 g/L) was ultrasonicated for 30 min and allowed to equilibrate overnight before use.

2.5. NMR experiments

^{1}H NMR spectra of the peptides were recorded in both D_2O and H_2O/D_2O mixture (90/10 v/v). Sample for interaction measurements contained 4 mg peptide and 1 mg linear polymer. TOCSY spectra (total correlation spectroscopy) were recorded on a Varian UNITY Plus 400 MHz NMR spectrometer at room temperature at a mixing time of 80 ms. Spectral width for both the F1 and the F2 dimension was 2873.6 Hz. Each collected data set contained 256 (t1) $\times$ 1024 (t2) data points. The data sets were linearly predicted to be 1024 $\times$ 1024 data points.

2.6. CD spectroscopy

Static CD (circular dichroism) spectra were recorded on a JASCO (Easton, MD) J-715 spectropolarimeter at 20 °C in H_2O. The CW-4 and VW-8 concentration was 40 mmol/L and 20 mmol/L, respectively. Ellipticity scans were collected in triplicate over 190–240 nm at 0.1 nm intervals, with a light path of 1 mm and a 1 s response time in a 1.0 cm quartz cell. Final spectra representing the plots of mean residue ellipticity ($[\theta]$) in deg cm^2/dmol vs. wavelength (λ) in nm were smoothed over an interval of five data points prior to plotting. The percentage helical content was estimated by the method of Yang [24].

2.7. ITC experiments

All ITC experiments were performed on a VP-ITC (Microcal) calorimeter between *l*-DMAPAM and peptides in H_2O at 298.15 K under atmospheric pressure with 45 successive injections. Solutions were degassed and thermostatted by a ThermoVac accessory before the titration. A constant volume (6 μL/injection) of the peptide solution (0.8 mM) in a 0.250 mL syringe was injected into the reaction cell (1.4227 mL) charged with the polymer solution

(0.05 mM). Dilution heat was determined by a blank experiment before each run with the injection of peptide into H_2O and was later subtracted to give net reaction heat. The ionic strength of the solution was adjusted by NaCl.

2.8. Molecular docking

DMAPAM docking to the peptides with different conformations was performed using the Autodock 3.0 program. In all cases lowest energy conformation was applied as the initial molecular conformation. Two repeating functional group units in DMAPAM were built as the adsorbent model by SYBYL 6.91 program package. The sketched molecular structure of DMAPAM was first optimized by 1000 iterations of molecular mechanics minimization using Powell's gradient algorithm method. The Tripos force field and the Gasteiger–Huckel charge were chosen. The default settings were used for the other parameters. Then the obtained conformation of DMAPAM was refined by simulated annealing method. The default setting was used except for atomic charges which were the Gasteiger–Huckel charge. The refined conformations of DMAPAM were optimized by molecular mechanics minimization again. A value of 0.05 kcal/mol for the gradient termination cutoff was selected. And the lowest energy conformation of DMAPAM was selected as the initial molecular conformation for docking. The α-helical conformation of VW-8 was built by Biopolymer Block in SYBYL 6.91 and optimized by molecular mechanics minimization. The random coil conformations of VW-8 and CW-4 were built by Stretch Block in SYBYL 6.91 and also optimized by molecular dynamics and molecular mechanics minimization. During the docking, the model DMAPAM was allowed to be flexible and move on the grid on the fixed peptides during docking. An initial population of 150 starting structures was used for energy optimization with a maximum energy evaluation of 10^7. Default parameters were applied except for grid spacing being 0.375 Å. Taking into account the size of each peptides, grid dimension was $5.0\ nm \times 6.0\ nm \times 5.8\ nm$, $5.4\ nm \times 5.0\ nm \times 4.8\ nm$ and $4.2\ nm \times 4.6\ nm \times 4.8\ nm$ for α-helix conformation of VW-8, random coil conformations of VW-8 and CW-4, respectively. Grid search was performed using the Lamarckian genetic algorithm. A total of 100 different docking runs were performed to find the best conformation and ligand orientation based on the binding energy. The SYBYL program package (TRIPOS Inc.) was used to display the conformations obtained during the docking.

2.9. SPR biosensor measurements

Kinetic binding measurements were performed on a BIAcore 3000 SPR measurement apparatus on CM5 chips. The peptides were immobilized on the chips by a conventional amine coupling in 10 mM sodium acetate (pH = 4.5) at a constant flow rate of 5 μL/min at 25 °C. A total of 284 RU VW-8 and 164 RU CW-4 were immobilized (RU: pg/mm^2, immobilized protein concentration [25]).

All the kinetic experiments were carried out at 25 °C at a flow rate of 10 μL/min in PBS buffer (pH = 7.4). In each run a total of 30 μL *l*-DMAPAM in PBS buffer of different concentrations was injected over the peptide-modified sensor surface for 3 min, followed by washing with PBS buffer for 5 min, 1 M NaCl for 1 min, and 0.02% SDS for 1 min. The binding and dissociation data were analyzed in a BIA evaluation Software version 4.1 with a nonlinear regression analysis of the measured sensorgrams among the following binding models: simple 1:1 (Langmuir) binding, two-state (conformation change) reaction, heterogenous ligand-paralleled reaction and bivalent analyte model. The reduced chi-square (χ^2) values were used to determine the goodness of the fit.

3. Results and discussion

In the present study, peptide VW-8 (NH_2–VVRGCTWW–COOH), which was separated from uremic sera in our previous work [22], is selected as the target molecule. Lowe and co-workers have been outlined three different approaches to design a synthetic affinity ligand [26]. The first approach is to use the known structure of a natural protein–ligand interaction as a template for a synthetic ligand. The second method is to design a ligand with the construction that displays complementarity to the target site. And the third approach is building up a direct mimicking of a natural biological recognition site. To any approach among them, Lowe suggested that the first stage for designing synthetic affinity ligands should be selection of a target site or investigation of a known biological interaction that could be used as a template for modeling [26]. According to our previous research, the main binding site between DMAPAM adsorbent and VW-8 was found to be the tryptophan on the C-terminus [23]. For further investigating the selectivity of adsorbent, the peptide CW-4 (NH_2–CTWW–COOH), a fragment of VW-8 also having tryptophan on the C-terminus, was selected as the reference peptide. As expected, DMAPAM also can adsorb CW-4 due to the presence of same binding site.

According to the data of adsorption experiments (Table 1), DMAPAM has high selectivity to VW-8 and CW-4. The data in Table 1 show that the adsorption capacity of adsorbents to CW-4 was rather low. In particular, the adsorption capacity to CW-4 was zero at pH 5.4. This observed drastic difference in adsorption could not be explained by the primary sequence of the peptide and electrostatic force, while many literatures reported that the adsorption selectivity was attributed to the binding site and charges [27–31].

Furthermore, dimethylamine modified linear polyacrylamide (*l*-DMAPAM) was prepared and found to also have a significantly stronger interaction with VW-8 than CW-4 by ITC. The linear polymer *l*-DMAPAM is soluble in H_2O and can serve as a viable model for the cross-linked adsorbent DMAPAM.

The study of isothermal titration calorimetry directly measured binding enthalpies to examine the interaction thermodynamics associated with the polymers and peptides. The data, therefore, provide further insight into the reversible, equilibrium binding processes established between peptides and polymers.

According to ITC results, the interaction of CW-4 to *l*-DMAPAM was significantly weaker than that of VW-8 (Fig. 2). The curve of CW-4 titrated into *l*-DMAPAM with an unfavorable enthalpy from the first to second injection, which was originated from dilution of peptide, was approximately accessed to zero. This demonstrated that there was no significant interaction between CW-4 and *l*-DMAPAM. While the curve of VW-8 titrated into *l*-DMAPAM with an obvious exothermic peak demonstrated a multi-step interaction between the polymer and the VW-8, because the one-step binding curve has a maximum binding from the first injection until saturation of binding sites.

3.1. Analysis of binding sites by 2D NMR spectroscopy

The TOCSY spectrum of CW-4 was recorded (Fig. 3) and the signals were assigned. Comparing ^{1}H NMR spectra of CW-4 itself

Table 1
Adsorption capacity of the adsorbents to peptides.

Peptide	Adsorption capacity (mg/g wet adsorbent)		
	pH = 4	pH = 5.4	pH = 9
VW-8	0.318 ± 0.012	0.541 ± 0.009	0.598 ± 0.017
CW-4	0.024 ± 0.004	~0 ± 0.002	0.045 ± 0.007

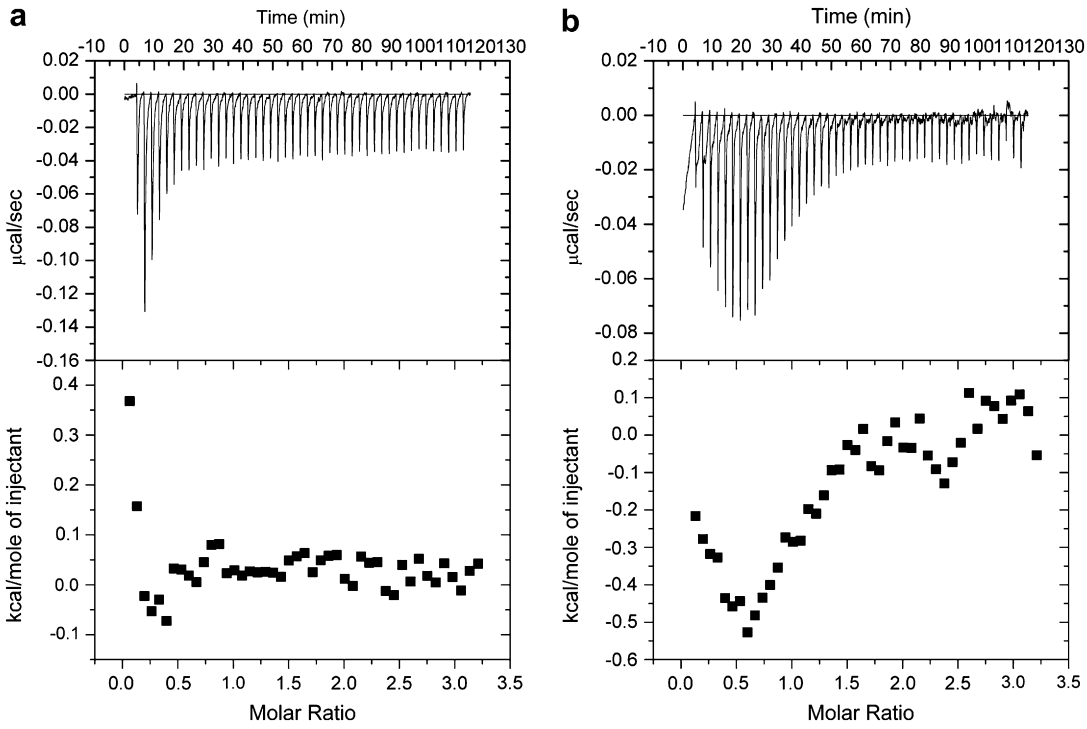

Fig. 2. ITC titration of CW-4 and VW-8 with *l*-DMAPAM. (a) The upper graphic was the raw data for sequential injections of CW-4 (0.8 mM) into *l*-DMAPAM (0.05 mM); the down graphic was the apparent reaction heat obtained from the integration of calorimetric traces. (b) The upper graphic was the raw data for sequential injections of VW-8 (0.8 mM) into *l*-DMAPAM (0.05 mM); the down graphic was the apparent reaction heat obtained from the integration of calorimetric traces.

and CW-4 with *l*-DMAPAM (Table 2), a slight change in chemical shift was observed for the NH signals of the terminal Trp. Although every residue in the flexible oligopeptide CW-4 has the opportunity to interact with *l*-DMAPAM without steric hindrance, only the signal from the terminal Trp was affected by the *l*-DMAPAM. This high specificity of the observed spectral change confirmed that the C-terminal Trp to be the binding site. The binding site between the VW-8 and the *l*-DMAPAM was also confirmed to be the terminal Trp, with the chemical shift changes of αH up to −0.12 ppm. (This has been reported in our previous paper [23].) These results demonstrated the binding site of CW-4 was same to that of VW-8. So the low adsorption of DMAPAM to CW-4 does not lie on the difference of binding site.

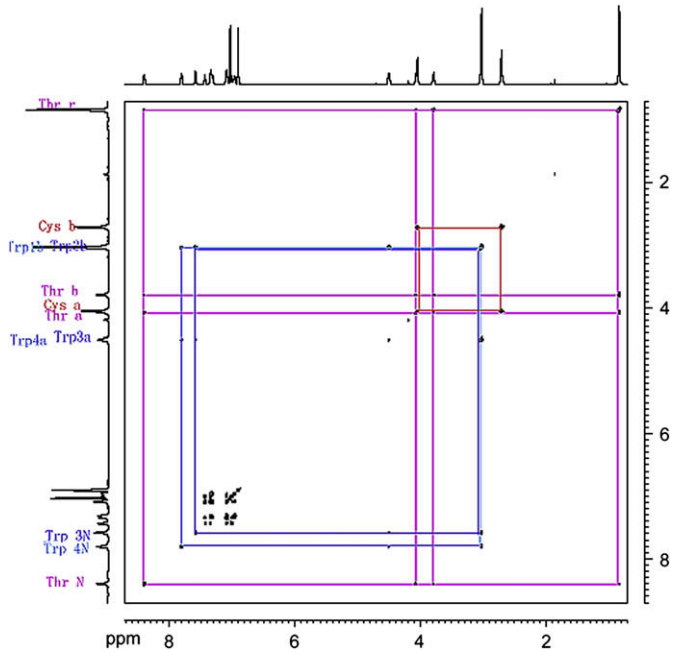

Fig. 3. TOCSY spectrum and assignment of CW-4. Letters a, b, N represent α proton, β proton and proton attached to nitrogen, respectively. Various color lines represent different selfspin systems. (For interpretation of the references to color in this figure legend, the reader is referred to the web version of this article.)

3.2. Electrostatic force

According to ITC results (Fig. 4), affinity between both oligopeptides and *l*-DMAPAM was weakened significantly by adding NaCl solution (100 mM) which neutralized the electrostatic interaction [32], thus, electrostatic force was considered to be the main driving force in the adsorption process. Nevertheless, compared with Fig. 2b, the exothermic peak changed to a gradual decreased endothermic curve when NaCl was added. At 100 mM salt concentration, most of the electrostatic interaction can be considered to be neutralized [33]. Furthermore, the ITC experiment was carried out in aqueous solution, the hydrogen bond could be interrupted by polar water molecules. However, in the ITC spectrum there was still interaction heat when VW-8 was titrated into

Table 2
Chemical shift of CW-4 and CW-4/*l*-DMAPAM.

Residue	δ NH (ppm)		δ αH (ppm)		δ βH (ppm)	
	CW-4	*l*-DMA[a]	CW-4	*l*-DMA	CW-4	*l*-DMA
Cys	–	–	4.05	4.05	2.71	2.71
Thr	8.41	8.41	4.08	4.08	3.79	3.79
Trp3	7.58	7.58	4.49	4.49	3.03	3.03
Trp4	7.82	7.80	4.51	4.51	3.03	3.03

[a] *l*-DMA represents H_2O–D_2O (9:1) solution of CW-4 that has been mixed with linear dimethylamine modified polyacrylamide.

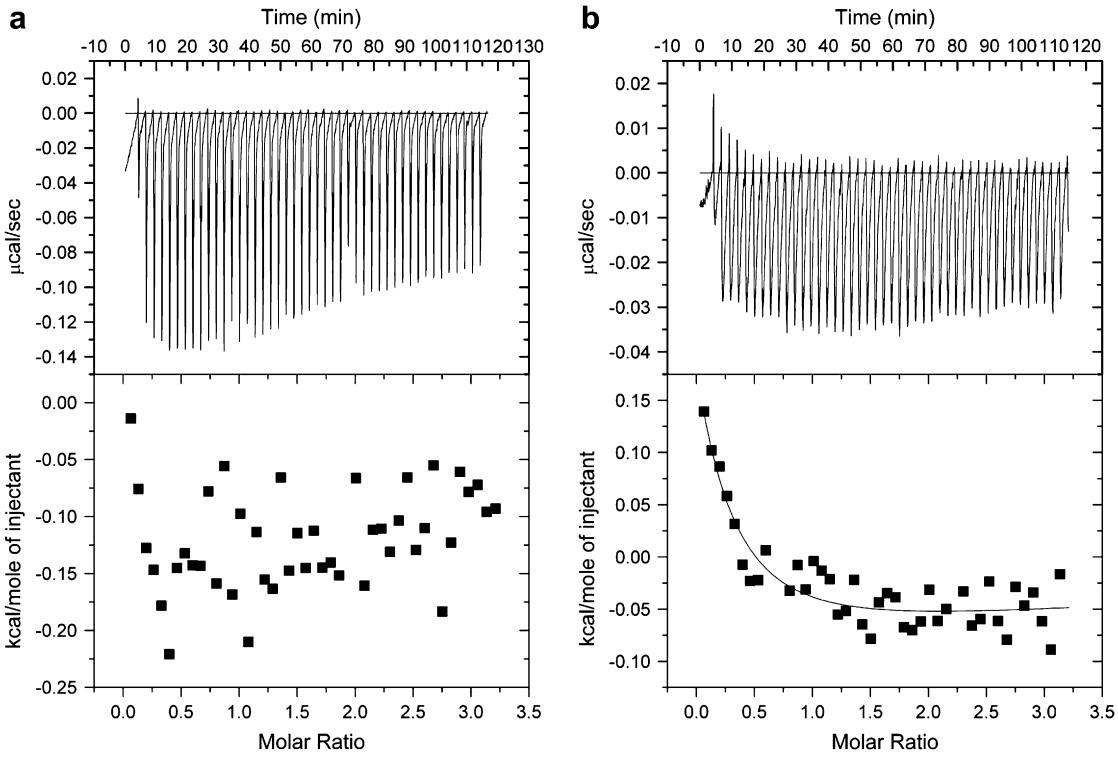

Fig. 4. ITC titration of CW-4 and VW-8 with *l*-DMAPAM in the presence of NaCl (100 mM). (a) The upper graphic was the raw data for sequential injections of CW-4 (0.8 mM) into *l*-DMAPAM (0.05 mM); the down graphic was the apparent reaction heat obtained from the integration of calorimetric traces. (b) The upper graphic was the raw data for sequential injections of VW-8 (0.8 mM) into *l*-DMAPAM (0.05 mM); the down graphic was the apparent reaction heat obtained from the integration of calorimetric traces.

DMAPAM solution. This means there was interactive force between the VW-8 and the DMAPAM except for electrostatic force.

Moreover, the isoelectric point (p*I*) of VW-8, CW-4 and *l*-DMAPAM determined by zeta potential measurement was 8.66, 5.22 and 8.33, respectively, suggesting that both VW-8 and *l*-DMAPAM were positively charged at pH 7, while CW-4 was negatively charged. However, according to ITC results, the interaction between the two positively charged species VW-8 and *l*-DMAPAM was significantly stronger than that of CW-4 and *l*-DMAPAM, which could not be accounted for electrostatic attraction. The attractive interaction between negatively charged bovine serum albumin (BSA) and polyanions has been reported by Tribet [33], but the attractive interaction between positively charged oligopeptide and polycations has not been reported to our knowledge. In Ref. [33], the attractive interaction between negatively charged BSA and polyanion was confirmed to be the hydrophobic interaction. In addition, the previous NMR results (Ref. [23]) referred the binding site between VW-8 and DMAPAM was the C-terminal Trp residue, and tryptophan has a hydrophobic indole group. So these results suggested that hydrophobic interaction exist between VW-8 and DMAPAM.

3.3. Determination of hydrophobic interaction

The hydrophobic interaction occurs when the hydrophobic motif of the ligand closes to the hydrophobic domain of the target molecule. So we could assess the hydrophobic interaction occurring according to the distance between the hydrophobic group on the

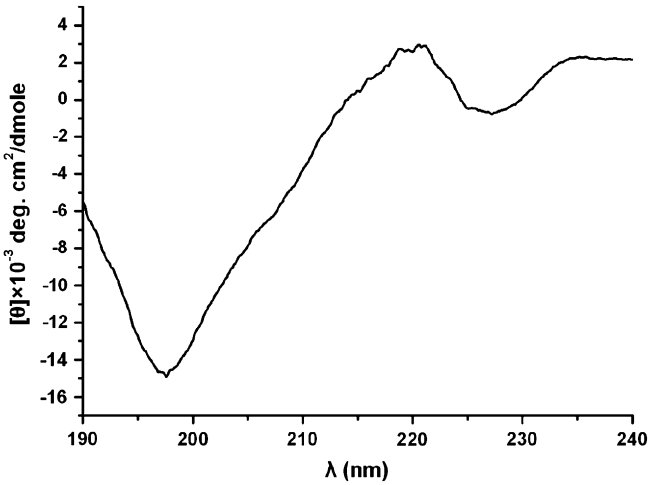

Fig. 5. CD spectra of CW-4 with random coil conformation in distilled H_2O at 20 °C.

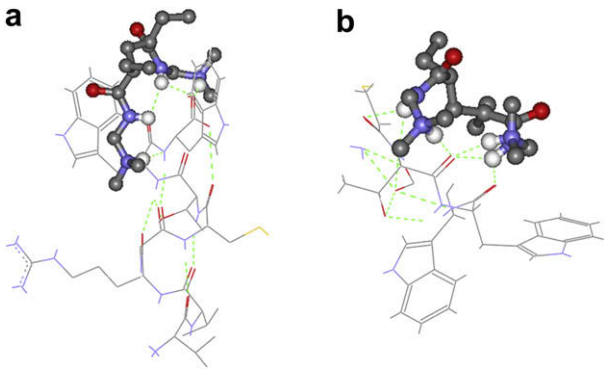

Fig. 6. The interaction model of DMAPAM docked to peptides using Autodock 3.0. (a) The best conformation of DMAPAM docked to α-helix conformation of VW-8. (b) The best conformation of DMAPAM docked to random coil conformation of CW-4.

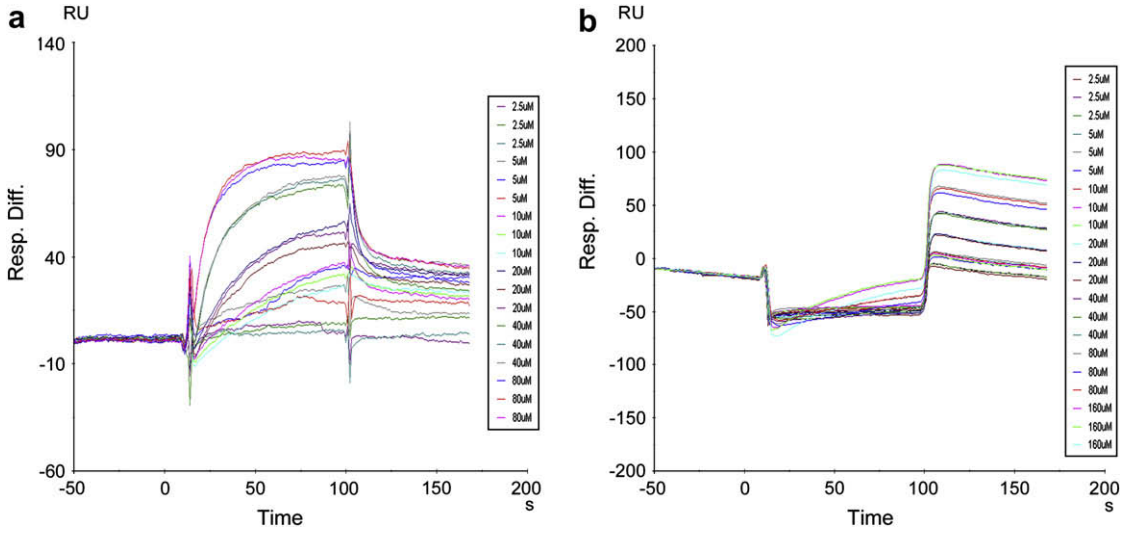

Fig. 7. The sensorgram data of the control sensorgram data subtracted from the peptide-modified sensorgram data with different concentrations of polymer solution. (a) The VW-8 modified sensorgram; (b) the CW-4 modified sensorgram.

peptide and the hydrophobic group on the adsorbents. NOESY (Nuclear Overhauser Effect Spectroscopy) spectra provide information about protons that are 5 Å or less apart in space. The information is through space and not through bond. The presence of an NOE peak is direct evidence that two protons are within 5 Å through space. Due to the solubility, the solvent is the mixture of DMSO and H_2O (v/v = 2:1), so TNNOESY (Nuclear Overhauser Effect Spectroscopy includes the option of water suppression with the transmitter) was used to investigate the interaction between VW-8 and *l*-DMAPAM. In the TNNOESY spectrum, besides the intramolecular cross-peaks of VW-8 itself, the intermolecular cross-peaks exactly between the indolyl protons (6.94 ppm) and the methyl protons (2.09 ppm) of the dimethylamide group were found (figure not shown). These results demonstrated that there occurred hydrophobic interaction between VW-8 and *l*-DMAPAM. However, the CW-4, possessing the identical Trp residues of VW-8, seemed not to interact via hydrophobic force if there were any interactions. Such differences suggested that other factors play significant and even primary roles other than hydrophobic forces, which awaited our further investigation.

The result of molecular docking provided the rational interpretation. We have previously established the helical conformation of VW-8 [23]. In the present work, random coil was the conformation of CW-4 as revealed by CD spectroscopy (Fig. 5) and chemical shift index. Effect of conformational difference on adsorption capacity is explored herein.

Molecular models of peptides with different conformations were built according to NMR and CD results. The α-helical conformation of VW-8 (Fig. 6a) showed that the two indole groups in the tryptophan residues formed a clamp structure with a dihedral angle of 72.9°. The minimum distance from one indole ring to the other was 0.495 nm. The maximum distance between two hydrogen atoms on two dimethyl groups in DMAPAM was 0.382 nm. The size of the clamp allowed the dimethylamine to insert into the hydrophobic gap between two tryptophans. In contrast, the two tryptophan residues on CW-4 (Fig. 6b) were extended in opposite direction due to stereoeffect. In addition, according to molecular docking, the average binding energy of CW-4 to DMAPAM is −27.05 kJ/mol, while the average binding energy of VW-8 in α-helix conformation to DMAPAM is −37.97 kJ/mol. Meanwhile, the binding energy of VW-8 in random coil conformation to DMAPAM was −28.73 kJ/mol. Evidently, the helical conformation of VW-8 was favored in the interaction between VW-8 and DMAPAM, and the best conformation of DMAPAM docked to peptides obtained by Autodock 3.0 (Fig. 6) showed the Trp residue was the binding site, in exact agreement with the NMR and ITC results. Therefore, aside from the electrostatic attraction between the tertiary amine on DMAPAM and carboxyl group of Trp residue, the interaction affinity of VW-8 gained benefit from the conformation dependent hydrophobically driven attractions to DMAPAM overriding Coulomb repulsion.

In contrast, the best conformation obtained by DMAPAM docked to random coil conformation of CW-4 showed the interaction mainly depended on hydrogen bonds (Fig. 6b), which would be severely weakened in aqueous solution.

Table 3
The χ^2 of residuals calculated by four possible kinetic models to globally fit the sensorgrams for the different peptides and *l*-DMAPAM interactions.

	Langmuir	Conformation change	Heterogenous	Bivalent
CW-4	41.1	41.1	42.7	41.1
VW-8	47.4	49.1	40.4	47.1

Four different kinetic models were a simple 1:1 (Langmuir) binding; a two-state (conformation change) reaction; a heterogenous ligand-paralleled reaction and a bivalent analyte model, respectively. The lowest χ^2 indicates the best fitting model.

3.4. Kinetic analysis

Peptides VW-8 and CW-4 were immobilized on SPR sensor chips and the chips were flushed by solutions of *l*-DMAPAM with different concentrations. Due to the relatively low affinity in peptide–polymer interaction compared with biological systems, during the binding stage, the amount of *l*-DMAPAM accumulated on CW-4 modified cell was even smaller than that of the control cell, giving a negative RU value. However, during the washing stage, the dissociation rate of *l*-DMAPAM from CW-4 modified cell is smaller than that of the control cell, and the net binding amount was calculated positive (Fig. 7). The binding curves of VW-8 and CW-4 indicated distinct interaction modes.

Four possible kinetic models were evaluated for the interaction modes between the peptides and the *l*-DMAPAM. All χ^2 residuals of the global fitting analysis for the two peptides binding to *l*-DMAPAM were presented (Table 3), and the heterogenous ligand-paralleled model was found the best fit to the interaction between VW-8 and *l*-DMAPAM. The interaction between VW-8 and *l*-DMAPAM

was suggested to be a complex kinetic process with more than two binding sites, consistent with NMR results and molecular docking. No obvious distinction was found among the χ^2 of different models for CW-4 and *l*-DMAPAM. Cooperating to the result of NMR, simple binding is the most possible mode of interaction.

Four different kinetic models were a simple 1:1 (Langmuir) binding; a two-state (conformation change) reaction; a heterogenous ligand-paralleled reaction and a bivalent analyte model, respectively. The lowest χ^2 indicates the best fitting model.

4. Conclusion

The interaction between oligopeptide and dimethylamine modified polyacrylamide adsorbent was investigated in detail via *l*-DMAPAM. With model system, the structural information of interaction was obtained by 2D ^{1}H NMR technique. The thermodynamic and kinetic data, particularly real-time monitored data were investigated by SPR and ITC. The results not only are in good agreement with the trend of adsorption experiments, but also revealed that the driving force is electrostatic force. Comprehensive analysis of binding site, driving force of binding and binding mode demonstrated the α-helix conformation of peptide VW-8 contributes to its high adsorption affinity toward the adsorbents, and the lack of such conformation in peptide CW-4 accounts for the significantly decreased affinity. The results suggest that the conformation difference of the two peptides has a great impact on the interaction mode and further affects the affinity between the peptides and the adsorbents.

According to the results of this paper, besides the special residues, designing synthetic affinity ligand for VW-8 must be considered the space construction of the two Trp residues. Without further investigation of the selectivity of VW-8 and CW-4 on adsorbent, the structural basis for designing affinity adsorbent could not be obtained. Moreover, linear polymers employed in this paper provide the possibility of studying the interaction mechanism on a molecular level, and several techniques which are difficult to study the interaction mechanism between targets and adsorbents have been used, for example, NMR, ITC and SPR.

Acknowledgements

J.L. and J.F. contributed equally to this work. This work was financially supported by the National Natural Science Foundation of China (Grant Nos. 20634030 and 50573034).

References

[1] Cuatrecasas P, Wilchek M, Anfinsen CB. Proc Natl Acad Sci USA 1968;61:636–43.
[2] Linhult M, Gülich S, Hober S. Protein Pept Lett 2005;12:305–10.
[3] Gao B, Wang J, An F, Liu Q. Polymer 2008;49:1230–8.
[4] Wang S, Yu Y, Cui T, Chen Y. Biomaterials 2003;24:2799–802.
[5] Gomez CG, Igarzabal CIA, Strumia MC. Polymer 2005;46:6300–7.
[6] Häußler M, Qin A, Tang BZ. Polymer 2007;48:6181–204.
[7] Peppas NA, Huang Y. Pharm Res 2002;19:578–87.
[8] Turner NW, Jeans CW, Brain KR, Allender CJ, Hlady V, Britt D. Biotechnol Prog 2006;22(6):1474–89.
[9] Fexby S, Bülow L. Trends Biotechnol 2004;22:511–6.
[10] Fassina G, Verdoliva A, Palombo G, Ruvo M, Cassani G. J Mol Recognit 1998;11:128–33.
[11] Palombo G, De Falco S, Tortora M, Cassani G, Fassina G. J Mol Recognit 1998;11:243–6.
[12] Xu JZ, Moon SH, Jeong B, Sohn YS. Polymer 2007;48:3673–8.
[13] Kaufman DB, Hentsch ME, Baumbach GA, Buettner JA, Dadd CA, Huang PY, et al. Biotechnol Bioeng 2002;77:278–89.
[14] Clonis YD, Lowe CR. J Chromatogr 1991;540:103–11.
[15] Li R, Dowd V, Stewart DJ, Burton SJ, Lowe CR. Nat Biotechnol 1998;16:190–5.
[16] Teng SF, Sproule K, Husain A, Lowe CR. J Chromatogr B Biomed Sci Appl 2000;740:1–15.
[17] Labrou NE, Karagouni A, Clonis YD. Biotechnol Bioeng 1995;48:278–88.
[18] Hart BR, Shea KJ. Macromolecules 2002;35:6192–201.
[19] Czerwenka C, Lammerhofer M, Maier NM, Rissanen K, Lindner W. Anal Chem 2002;74:5658–66.
[20] Rachkov A, Minoura N. Biochim Biophys Acta 2001;1544:255–66.
[21] Shiomia T, Matsuia M, Mizukamib F, Sakaguchi K. Biomaterials 2005;26:5564–71.
[22] Chu JG, Yuan Z, Liu XH, Wu Q, Mi HF, He BL. Clin Chim Acta 2001;311:95–107.
[23] Li GH, Li JH, Wang W, Yang M, Zhang YW, Sun PC, et al. Biomacromolecules 2006;7:1811–8.
[24] Yang JT, Wu CC, Martinez HM. Methods Enzymol 1986;130:208–69.
[25] Stenberg E, Persson B, Roos H, Urbaniczky C. J Colloid Interface Sci 1991;143:513–26.
[26] Lowe CR, Lowe AR, Gupta G. J Biochem Biophys Methods 2001;49:561–74.
[27] Serizawa T, Sawada T, Kitayama T. Angew Chem 2007;119:737–40.
[28] Renner C, Piehler J, Schrader T. J Am Chem Soc 2006;128:620–8.
[29] Phillips DC, York RL, Mermut O, McCrea KR, Ward RS, Somorjai GA. J Phys Chem C 2007;111:255–61.
[30] Roy R, Sandanaraj BS, Klaikherd A, Thayumanavan S. Langmuir 2006;22:7695–700.
[31] Szumski M, Klodzińska E, Jarmalavičienė R, Maruška A, Buszewski BJ. Biochem Biophys Methods 2006;70:107–15.
[32] Thomas CJ, Surolia A. FEBS Lett 1999;445:420–4.
[33] Tribet C, Porcar I, Bonnefont PA, Audebert R. J Phys Chem B 1998;102:1327–33.

Abbreviations

ITC:	isothermal titration calorimetry
SPR:	surface plasmon resonance
NMR	nuclear magnetic resonance
TOCSY:	total correlation spectroscopy
CD:	circular dichroism spectra
TNNOESY:	Nuclear Overhauser Effect Spectroscopy includes the option of water suppression with the transmitter
VW-8:	NH_2–VVRGCTWW–COOH
CW-4:	NH_2–CTWW–COOH
PAM:	polyacrylamide
DMAPAM:	dimethylamine modified polyacrylamide
l-DMAPAM:	dimethylamine modified linear polyacrylamide